Landing Trajectory Prediction for UAS Based on Generative Adversarial Network

Jun Xiang[*], Drake Essick[†] , Luiz Gonzalez Bautista[‡], Junfei Xie [§], Jun Chen[¶]
San Diego State University, San Diego, CA 92182

Models for trajectory prediction are an essential component of many advanced air mobility studies. These models help aircraft detect conflict and plan avoidance maneuvers, which is especially important in Unmanned Aircraft systems (UAS) landing management due to the congested airspace near vertiports. In this paper, we propose a landing trajectory prediction model for UAS based on Generative Adversarial Network (GAN). The GAN is a prestigious neural network that has been developed for many years. In previous research, GAN has achieved many state-of-the-art results in many generation tasks. The GAN consists of one neural network generator and a neural network discriminator. Because of the learning capacity of the neural networks, the generator is capable to understand the features of the sample trajectory. The generator takes the previous trajectory as input and outputs some random status of a flight. According to the results of the experiences, the proposed model can output more accurate predictions than the baseline method(GMR) in various datasets. To evaluate the proposed model, we also create a real UAV landing dataset that includes more than 2600 trajectories of drone control manually by real pilots.

I. Introduction

Unmanned aerial vehicles (UAVs) are the future of aviation. FAA forecasts that there will be 1.81 million units of drone fleet by 2026 [1]. With so many UAVs flying in the airspace, tracking and predicting the motion of UAVs become important. The security service needs to predict misused drones in public areas including airports, mass events, or public demonstrations [2]. Meanwhile, in-network UAVs need to predict the trajectory of out-network UAVs to avoid them, which is especially important in UAV landing management due to the congested airspace near vertiports [3]. Conflict detection and resolution(CD&R) technology, plays an important role in the air traffic system [4,5] and highly relies on accurate and timely predictions of out-network UAV trajectories [6]. There are many methods have been proposed to predict the trajectory of UAVs. However, existing methods for UAV trajectory prediction are ordinarily very slow and unable to be applied online [7]. In addition to fast prediction, higher accuracy of prediction results is required. Many planning methods are bothered by the uncertainty of the future prediction.

Aircraft trajectory prediction is always a popular research topic and there are many methods proposed. The Recurrent Neural network is proposed to predict aircraft trajectory with weather features [8]. The Hidden Markov Model (HMM) is recently applied to predict trajectories considering environmental uncertainties [9]. The deep generative convolutional recurrent neural network (RNN) approach is applied for 4D trajectory prediction [10]. A hybrid 3-dimensional UAV modeling framework, which integrates the physics-based and data-based models, can predict the motion of UAVs using only a small amount of real fight data [11]. Some aircraft prediction methods focus on modeling aircraft trajectories around the terminal. One traditional way is to predict the aircraft near the terminal by the Physical equation of motion [12]. The bayesian network can learn statistical representations of dynamic variables of aircraft and predict the motion [13]. Probabilistic generative model [14] predicts the aircraft trajectory by learning from position measurements.

The neural network generator has been proven to predict many objects such as language, image, and trajectories of pedestrians. Transformer [15] is the state-of-the-art method to draw global dependencies between input and output. BERT [16], uses Transformer as one of the encoders and is able to understand and process natural language. GATs [17] achieved the state-of-the-art result across four established transductive and inductive graph benchmarks leveraging masked self-attentional layers. At the same time, the transformer has successfully been used with GANs. SAGAN [18] achieved pioneering image generation results by using a transformer layer in GANs. ViTGAN [19]achieves a comparable performance of image generation to state-of-the-art CNN-based GANs without using convolution or pooling.

---

[*]Ph.D. Student, Department of Aerospace Engineering, AIAA Student Member, `jxiang9143@sdsu.edu`

[†]Undergraduate student, Department of Electrical and Computer Engineering, `dessick3793@sdsu.edu`

[‡]Undergraduate student, Department of Electrical and Computer Engineering, `lgonzalezbauti4071@sdsu.edu`

[§]Associate Professor, Department of Electrical and Computer Engineering, AIAA Member, `jxie4@sdsu.edu`

[¶]Assistant Professor, Department of Aerospace Engineering, AIAA Senior Member, `Jun.Chen@sdsu.edu`

CNN also performs decently recognizing image and text [20, 21] [22, 23]. GANs have proven to be able to capture the movement of mobile objects and predict their trajectories in many existing studies. For example, Social-GAN [24] is able to predict pedestrians' movement considering the social interaction between pedestrians. SoPhie [25] can understand the scene context besides social behavior and generate pedestrian trajectories. CGAN was proposed in [26] to solve weather-related aircraft trajectory prediction problems. 3D-GAN [27] can generate high-quality 3D objects without supervision. Therefore it is rational to train a Neural network to predict the landing trajectory of the UAS.

The paper proposes to predict the landing trajectory for UAS with a GAN-based method. The major contributions of this paper are summarized as follows:

- This paper adopts a 2D trajectory GAN-based method to predict 3D landing trajectories of UAS. The proposed method can generate prediction very fast and outperform the Gaussian Mixture Regression(GMR) in accuracy.

- This paper provides a real UAS landing trajectory dataset for future research.

- After GANs are well-trained, the discriminator part can be used to evaluate other predictions.

The paper's structure is as follows. Section II explains the background of GANs and GMM; Section III introduces the trajectory, how the dataset is created, and the architecture of the generator; Section IV shows the results by comparing the GANs and GMM; Section V concludes this paper.

II.   Background

A.   LSTM Generative Adversarial Network

Long Short-Term Memory (LSTM) [28] is a novel recurrent network architecture in conjunction with an appropriate gradient-based learning algorithm. The LSTM can enforce constant error flow so it can accelerate learning store information over extended time intervals. LSTM consists of multiplicative gate units that can learn to open or close the access to the error flow. LSTM can be used as the encoder and the decoder in GANs.

A Generative Adversarial Network consists of two neural networks, generator and discriminator, trained in opposition to each other [29]. The training procedure is similar to a two-player min-max game with the following objective function:

$$\min_G \max_D V(D, G) = \mathbb{E}_{x \sim p_{data}(x)}[\log D(x)] + \mathbb{E}_{z \sim p_z(z)}[\log 1 - D(G(z))] \tag{1}$$

In this paper, G denotes the generator that inputs factors and generates trajectory. z denoted the input factors that decide how a flight should fly. Generator G takes the input factors and output trajectory G(z). D denotes discriminator and D(x) output the probability that x is a trajectory is desired.

Gupta proposed social-GAN [24] that can understand human motion behavior. The social-GAN is able to observe the motion trajectories of pedestrians and predict the trajectories of pedestrians. Social-GAN combines tools from sequence prediction and generative adversarial networks. The generator of the social-GAN is consists of an LSTM-based encoder, a pooling module, and an LSTM-based decoder. The LSTM encoder encodes the motion trajectories to hidden items h. Then the pooling module pool the hidden items h while combining desired information i and the hidden items h together. Finally, the decoder decodes the hidden items and outputs the predicted trajectory.

B.   Gaussian Mixture Regression predictor

In this paper, Gaussian Mixture Regression(GMR) predictor is the baseline method. GMR predictor was proposed in [30] and the GMR predictor we use in this paper is proposed in [31]. The GMR predictor is one of the most popular predictors. The training process of GMR is shown as equation (2).

$$p(\boldsymbol{x}, \boldsymbol{y}) = \sum_{k=1}^{K} \pi_k \mathcal{N}_k \left(\boldsymbol{x}, \boldsymbol{y} \mid \boldsymbol{\mu}_{\boldsymbol{xy}_k}, \boldsymbol{\Sigma}_{\boldsymbol{xy}_k} \right) \tag{2}$$

where $\mathcal{N}_k \left(\boldsymbol{x}, \boldsymbol{y} \mid \boldsymbol{\mu}_{\boldsymbol{xy}_k}, \boldsymbol{\Sigma}_{\boldsymbol{xy}_k} \right)$ are Gaussian distributions with mean $\boldsymbol{\mu}_{\boldsymbol{xy}_k}$ and covariance $\boldsymbol{\Sigma}_{\boldsymbol{xy}_k}$, K is the number of Gaussians, and $\pi_k \in [0, 1]$ are priors that sum up to one.

After the GMR is trained, GMR predicts distributions of variables $\boldsymbol{y}$ by computing the conditional distribution $p(\boldsymbol{y} \mid \boldsymbol{x})$. The conditional distribution of each individual Gaussian

$$\mathcal{N}\left(\boldsymbol{x}, \boldsymbol{y} \mid \boldsymbol{\mu}_{xy}, \boldsymbol{\Sigma}_{xy} \right) \boldsymbol{\mu}_{xy} = \begin{pmatrix} \mu_x \\ \mu_y \end{pmatrix}, \quad \boldsymbol{\Sigma}_{xy} = \begin{pmatrix} \boldsymbol{\Sigma}_{xx} & \boldsymbol{\Sigma}_{xy} \\ \boldsymbol{\Sigma}_{yx} & \boldsymbol{\Sigma}_{yy} \end{pmatrix} \tag{3}$$

American Institute of Aeronautics and Astronautics

is defined by

$$\mu_{y|x} = \mu_y + \Sigma_{yx}\Sigma_{xx}^{-1}(x - \mu_x) \tag{4}$$

$$\Sigma_{y|x} = \Sigma_{yy} - \Sigma_{yx}\Sigma_{xx}^{-1}\Sigma_{xy} \tag{5}$$

the conditional distribution of each individual Gaussian and their priors is computed by equation

$$\pi_{y|x_k} = \frac{\mathcal{N}_k(x \mid \mu_{xk}, \Sigma_{xk})}{\sum_{l=1}^{K} \mathcal{N}_l(x \mid \mu_{xl}, \Sigma_{xl})} \tag{6}$$

to obtain the conditional distribution

$$p(y \mid x) = \sum_{k=1}^{K} \pi_{y|x_k} \mathcal{N}_k\left(y \mid \mu_{y|x_k}, \Sigma_{y|x_k}\right) \tag{7}$$

III.   Method

A.   Trajectory

Mathematically, Let T denotes the trajectory sequence of consists of multiple flight statuses. Let $x_{t+1} \in R^n$ the flight status at $t + 1$, will be determined by the previous status, dynamic model, and control input according to ordinary differential equation (ODE):

$$T_{t_1,t_2} = [x_{t_1}, x_{t_1+1}, ...x_{t_2-1}, x_{t_2}] \tag{8}$$

$$x_{t+1} = f(x_t, a_t(E)), a_t \in \mathbb{A} \tag{9}$$

where f denotes flight the dynamic model. a_t, denotes the control inputs which how the pilot reacts the environment E at time t. Let $a(E)$ called action function in these paper. $\mathbb{A}$ denotes the set of all the possible control inputs. However, in real world, flight dynamic model has noises and high computational cost. On the other hands, environment factors and previous status are only variables required to derive a trajectory. In this paper, the only flight status we focus on is position.

In order to predict the future trajectory without flight dynamic model and action function, the generator model(G) was proposed:

$$T_{t_1,t_2} = G(T_{t_0,t_1}) \tag{10}$$

where the Generator takes the previous trajectory sequence as input and outputs a predicted trajectory sequence. In this paper, all the previous trajectory sequence contains 10 points, and all the predicted trajectory sequence contains 10 points as well.

B.   Data Collection

In this paper, we prepare three different types of datasets to train the proposed model and test the learning capacity.

1.   Vertical Landing Data

We will start with a sample dataset as shown in Figure 1 to test how the generator works. The dataset includes the trajectories starting from four different directions to the destination (0,0,0). The average initial position is (-200, 200, 75) for direction1, (200, -200, 75) for direction2, (-200, -200, 75) for direction3, and (200, 200, 75) for direction4. The variance for the x, and y positions is 50, and for the z position is 3.5. The drone first flies horizontally to the points right above the destination, then land vertically.

2.   Linear Landing Data

The second dataset (as shown in Figure 2) we used to evaluate this method is simulated linear landing data. Same as vertical data, the drone flies from four different initial positions and land at position (0,0,0). The average initial position is (-400, 400, 140) for direction1, (400, -400, 140) for direction2, (-400, -400, 140) for direction3, and (400, 400, 140) for direction4. The variance for the x, and y positions is 100, and for the z position is 7.5. In contrast to vertical landing, the drone flight flies straight forward to the destination.
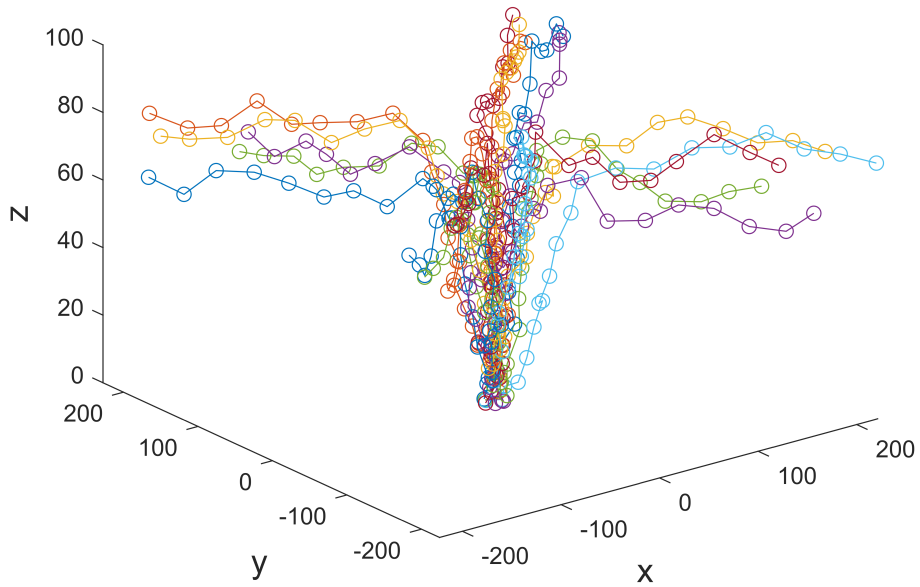
vertical landing

Figure 1: Vertical Landing Trajectory
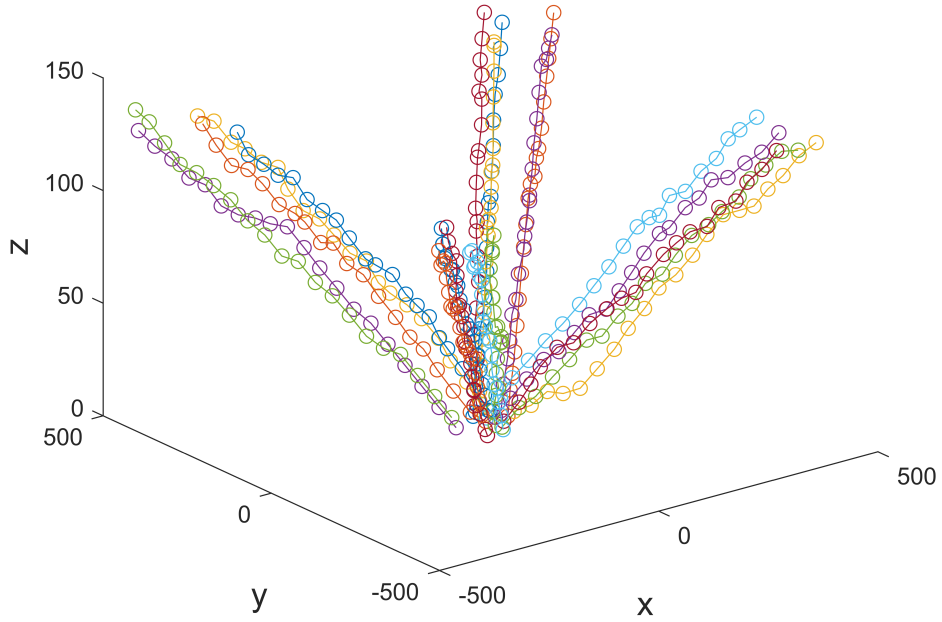
linear landing

Figure 2: Linear Landing Trajectory

3. Real Data

Real trajectories as shown in Figure 3 will be collected by the real pilot. Similar to the simulated data, the real pilot flies the drone from different initial positions and land at the destination. The initial position and trajectory pattern will fully rely on how the real pilot wants to control the drone. In this paper, the drone, as shown in Figure 4, is a customized DJI Tello, which we can track and localize by the motion capture system.
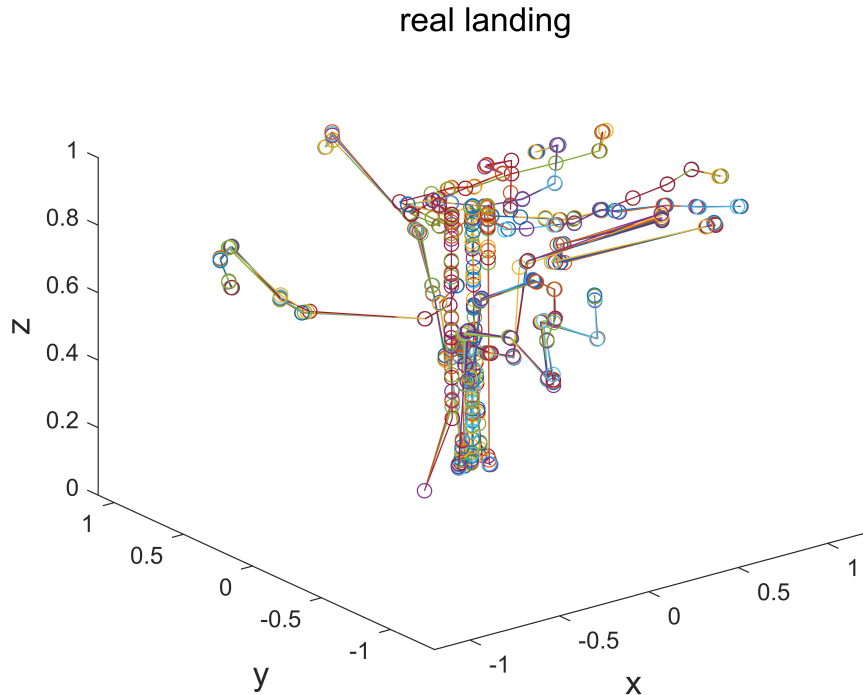

Figure 3: Real Landing Trajectory

Figure 4: DJI Tello Drone

C. LSTM-Pooling based Generator

The trajectory can be treated as a kind of data sequence, therefore, LSTM, which is one of the best neural network structures to understand data sequences, can be used to understand and generate the trajectory. Social-GANs [24] was proposed to predict pedestrians' future trajectory based on their past trajectory and social interaction. Similar to

social-GANs, We show one of the trajectories that are desired by the LSTM and tell LSTM some factors, then the LSTM generates trajectories based on the trajectory we showed to it.

The sequence data are needed to be embedded into a fixed-length vector before sending it into the LSTM cell. The LSTM cell will encode the embedded vector and previous hidden item into a current hidden item.

$$e_t = \sigma(x_t) \tag{11}$$

$$h_t^{el} = LSTM_{encoder}(h_{t-1}^{el}, e_t; W_{encoder}) \tag{12}$$

where e_t denotes the embedding vector. x_t is one of the flight statuses in the trajectory sequence. σ is the preprocessing function. h_t is the hidden time for time t. The W_{LSTM} is the LSTM weight. The pooling will input the environment factors and combine them into hidden items come from the LSTM encoder layer:

$$p = P(E, z) \tag{13}$$

$$e_t = \phi(x_{t-1}; W_{em}) \tag{14}$$

The the LSTM decoder layer will take the combined hidden item, generate the trajectory.

$$h_t^{dl} = LSTM_{decoder}(\gamma(h_{t-1}^{dl}, p), e_t; W_{decoder}) \tag{15}$$

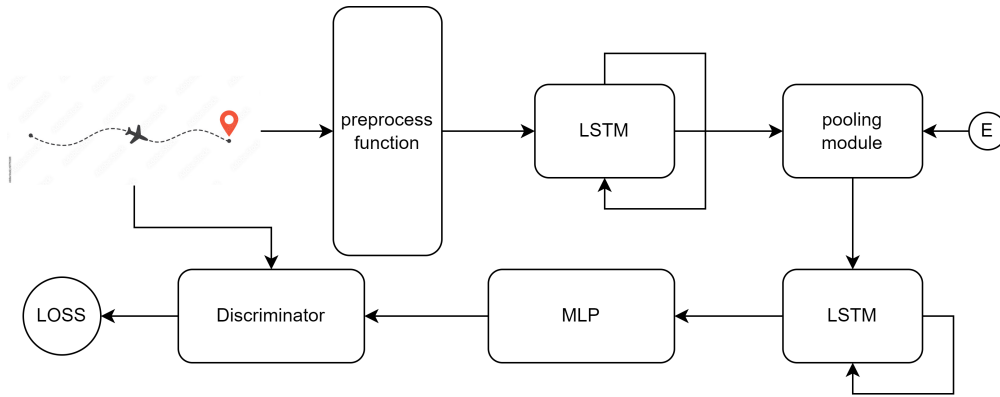$$x_t = \gamma(h_t^{dl}) \tag{16}$$

Figure 5: Training Process

D. Discriminator

Instead of a traditional mathematical model, we use a neural network as a discriminator to evaluate the generated trajectory. Based on the author's knowledge, there is no traditional mathematical model that is completely able to identify if a trajectory is a good trajectory. The discriminator inputs the trajectory T and gives a score s. If the given data is real, the discriminator is expected to give a high score. The score s is the main component of the loss function of the generator. In this paper, the discriminator is an LSTM network.

$$s = LSTM(T) \tag{17}$$

IV.   Result

The proposed GANs will be tested in three prepared datasets introduced in section B. For each dataset, there will be 3000(2430 for real) trajectories for training and 100 trajectories for evaluation. Figure 6,7 shows examples of the GMR and GAN predicting the landing trajectory. The accuracy of the prediction will be evaluated by the Average Displacement Error(ade) between the predicted trajectory and the real trajectory. Then, we will test if the discriminator can distinguish good and bad predictions.
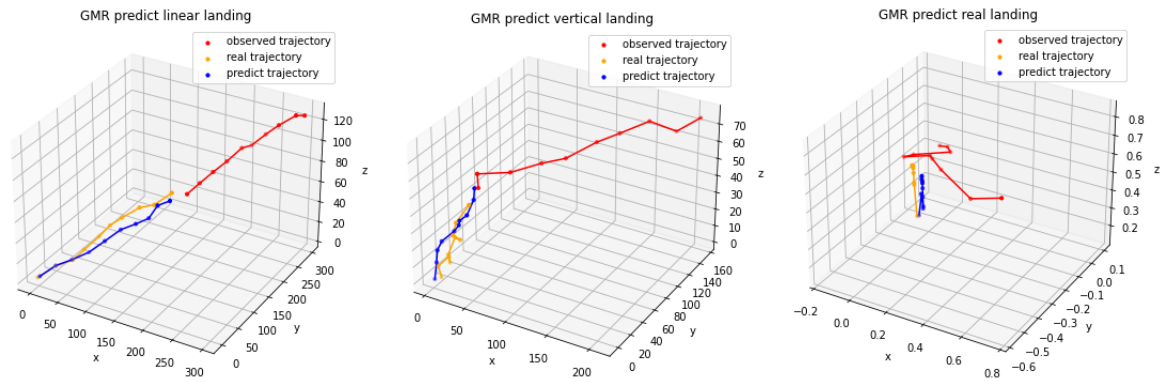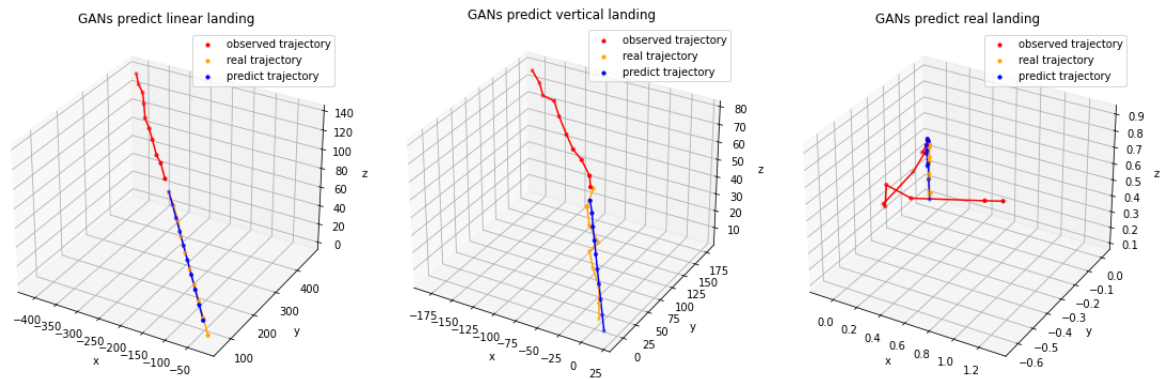
Figure 6: GMM prediction
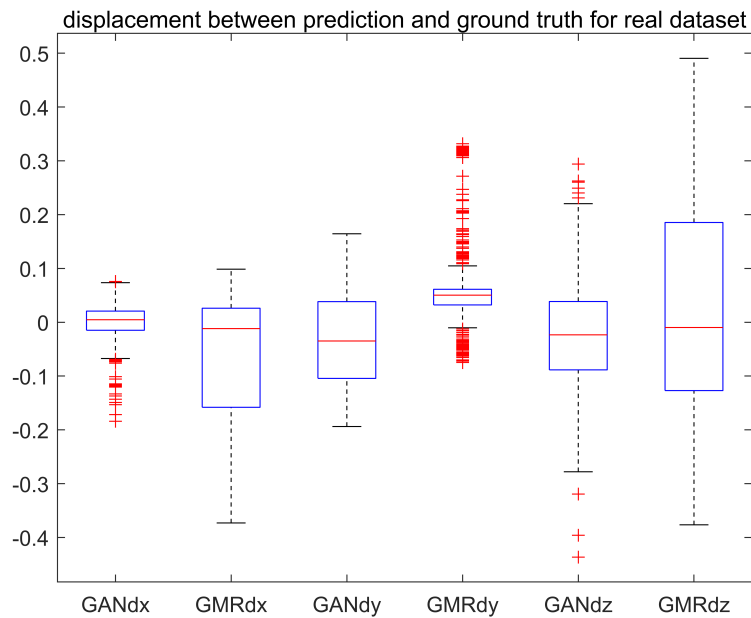

Figure 7: GANs prediction

Figure 8: prediction displacement in each axis(real dataset)

A. Average Displacement Error performance

The equation to calculate ade for one point is shown as equation 18

$$ade = mean(\sqrt{(dx)^2 + (dy)^2 + (dz)^2})$$ (18)

where dx is the displacement between the predicted point and the ground truth point in the x-axis, dy is the displacement in the y-axis and dz is the displacement in the z-axis. The trained GAN and GMR observe 100 evaluation trajectories and predict possible trajectories. The ade is the mean of 100 displacement errors between prediction and ground truth. The ade result for each point and the dataset is shown as tabel 1. The results show that GAN has a very good performance to predict the first four points, while the predicts get worse as the trajectory gets longer. For the vertical and linear datasets, GAN only outperforms GMR for the first four points. However, for the real dataset, GAN outperforms GMR for all the points. Because the vertical and linear dataset is simulated and has a smaller variance, it is easier for GMR, which is a Gaussian-based method, to predict. In contrast, in the real dataset, real pilots control the drone more randomly and the control logic is more subtle, GAN is able to mine the hidden rules and gets better results. Figure 8 shows a comparison of the prediction displacement in each axis for the real dataset between GAN and GMR. The displacement of GMR predictions obviously larger than GAN in all axes. In conclusion, GAN has much better accuracy in predicting the trajectories from the real dataset, while performing decently in predicting the trajectories from the simulated dataset. However, the longer the predicting is, the worse the GAN will perform.

Table 1: Average Displacement Error for each point(lower is better)

	vertical		linear		real	
method	GAN	GMR	GAN	GMR	GAN	GMR
point1	7.13±2.13	8.61±3.53	5.01±2.25	6.17±2.51	0.10±0.05	0.15±0.06
point2	9.11±4.2	11.12±4.87	7.31±3.44	9.1 ±3.86	0.11±0.04	0.18±0.07
point3	10.83±4.96	12.49±5.52	8.93±4.55	10.05±4.5	0.11±0.03	0.22±0.09
point4	12.11±5.56	14.04±5.73	10.4±5.33	11.28±5.19	0.12±0.03	0.23±0.12
point5	12.99±5.92	14.3±5.81	11.88±6.12	11.72±5.25	0.13±0.04	0.23±0.09
point6	13.44±6.32	14.19±5.67	12.67±6.4	12.57±6.13	0.14±0.04	0.23±0.11
point7	14.79±6.76	13.99±5.69	14.07±6.51	12.45±5.69	0.15±0.05	0.23±0.1
point8	15.06±7.09	12.52±5.81	14.97±7.68	12.27±5.41	0.14±0.06	0.24±0.1
point9	15.02±6.97	10.92±4.07	16.04±8.53	11.46±5.62	0.14±0.07	0.21±0.16
point10	14.88±8.41	9.0±3.69	17.01±8.97	10.93±5.72	0.18±0.08	0.24±0.21

B. Discriminator

The discriminator of the GANs can evaluate a trajectory and give a score. We show the discriminator 100 true trajectories and 100 fake trajectories from each dataset and let the discriminator generates the scores for those trajectories. The results are shown as table 2. According to the result, the discriminator gives higher scores to the true trajectories. It proves that the discriminator can distinguish true and fake trajectories.

Table 2: score given to real and fake trajectories by the discriminator

	vertical		linear		real	
method	True	Fake	True	Fake	True	Fake
score	2.79±0.31	-9.7±0.43	2.99±0.77	-7.93±0.67	2.32±2.76	0.21±0.86

V. Conclusion

In this paper, the LSTM-GAN-based method can accurately predict the motion of UAVs during the landing. The prediction error is lower than the baseline method. Meanwhile, the discriminator can give a high score to ground truth trajectories while giving a low score to fake trajectories. It proves that the trained discriminator can be used to evaluate the prediction. A dataset that includes a large number of trajectories of UAVs controlled by real pilots is also created. However, according to the results, the accuracy of prediction results becomes lower as the prediction length is longer.

This method may not work for long-term prediction. In the future, a new neural network encoder and decoder, which can process a larger amount of information is required for this GANs framework.

References

[1] FAA, "The Federal Aviation Administration (FAA) Aerospace Forecast Fiscal Years (FY) 2020-2040," 2020.

[2] Laurenzis, M., Rebert, M., Schertzer, S., Bacher, E., and Christnacher, F., "Prediction of MUAV flight behavior from active and passive imaging in complex environment," *Laser Radar Technology and Applications XXV*, Vol. 11410, SPIE, 2020, pp. 10–17.

[3] Zhou, Z., Chen, J., and Liu, Y., "Optimized landing of drones in the context of congested air traffic and limited vertiports," *IEEE Transactions on Intelligent Transportation Systems*, Vol. 22, No. 9, 2020, pp. 6007–6017.

[4] Lin, C. E. and Lai, Y.-H., "UAV path prediction for CD&R to manned aircraft in a confined airspace for cooperative mission," *International Journal of Aerospace Engineering*, Vol. 2018, 2018.

[5] Wu, P., Yang, X., Wei, P., and Chen, J., "Safety Assured Online Guidance With Airborne Separation for Urban Air Mobility Operations in Uncertain Environments," *IEEE Transactions on Intelligent Transportation Systems*, Vol. 23, No. 10, 2022, pp. 19413 – 19427.

[6] Kang, C. and Woolsey, C. A., "Model-based path prediction for fixed-wing unmanned aircraft using pose estimates," *Aerospace Science and Technology*, Vol. 105, 2020, pp. 106030.

[7] Xie, G. and Chen, X., "Efficient and robust online trajectory prediction for non-cooperative unmanned aerial vehicles," *Journal of Aerospace Information Systems*, Vol. 19, No. 2, 2022, pp. 143–153.

[8] Pang, Y., Yao, H., Hu, J., and Liu, Y., "A recurrent neural network approach for aircraft trajectory prediction with weather features from sherlock," *AIAA Aviation 2019 Forum*, 2019, p. 3413.

[9] Ayhan, S. and Samet, H., "Aircraft trajectory prediction made easy with predictive analytics," *Proceedings of the 22nd ACM SIGKDD International Conference on Knowledge Discovery and Data Mining*, 2016, pp. 21–30.

[10] Liu, Y. and Hansen, M., "Predicting aircraft trajectories: a deep generative convolutional recurrent neural networks approach," *arXiv preprint arXiv:1812.11670*, 2018.

[11] Wang, B., Xie, J., Wan, Y., Guijarro Reyes, G. A., and Garcia Carrillo, L. R., "3-d trajectory modeling for unmanned aerial vehicles," *AIAA Scitech 2019 Forum*, 2019, p. 1061.

[12] Chatterji, G., "Short-term trajectory prediction methods," *Guidance, Navigation, and Control Conference and Exhibit*, 1999, p. 4233.

[13] Kochenderfer, M. J., Edwards, M. W., Espindle, L. P., Kuchar, J. K., and Griffith, J. D., "Airspace encounter models for estimating collision risk," *Journal of Guidance, Control, and Dynamics*, Vol. 33, No. 2, 2010, pp. 487–499.

[14] Barratt, S. T., Kochenderfer, M. J., and Boyd, S. P., "Learning probabilistic trajectory models of aircraft in terminal airspace from position data," *IEEE Transactions on Intelligent Transportation Systems*, Vol. 20, No. 9, 2018, pp. 3536–3545.

[15] Vaswani, A., Shazeer, N., Parmar, N., Uszkoreit, J., Jones, L., Gomez, A. N., Kaiser, Ł., and Polosukhin, I., "Attention is all you need," *Advances in neural information processing systems*, 2017, pp. 5998–6008.

[16] Devlin, J., Chang, M.-W., Lee, K., and Toutanova, K., "Bert: Pre-training of deep bidirectional transformers for language understanding," *arXiv preprint arXiv:1810.04805*, 2018.

[17] Veličković, P., Cucurull, G., Casanova, A., Romero, A., Lio, P., and Bengio, Y., "Graph attention networks," *arXiv preprint arXiv:1710.10903*, 2017.

[18] Zhang, H., Goodfellow, I., Metaxas, D., and Odena, A., "Self-attention generative adversarial networks," *International conference on machine learning*, PMLR, 2019, pp. 7354–7363.

[19] Lee, K., Chang, H., Jiang, L., Zhang, H., Tu, Z., and Liu, C., "Vitgan: Training gans with vision transformers," *arXiv preprint arXiv:2107.04589*, 2021.

[20] Long, J., Shelhamer, E., and Darrell, T., "Fully convolutional networks for semantic segmentation," *Proceedings of the IEEE conference on computer vision and pattern recognition*, 2015, pp. 3431–3440.

[21] Ren, S., He, K., Girshick, R., and Sun, J., "Faster r-cnn: Towards real-time object detection with region proposal networks," *Advances in neural information processing systems*, Vol. 28, 2015, pp. 91–99.

[22] He, K., Zhang, X., Ren, S., and Sun, J., "Deep residual learning for image recognition," *Proceedings of the IEEE conference on computer vision and pattern recognition*, 2016, pp. 770–778.

[23] Huang, G., Liu, Z., Van Der Maaten, L., and Weinberger, K. Q., "Densely connected convolutional networks," *Proceedings of the IEEE conference on computer vision and pattern recognition*, 2017, pp. 4700–4708.

[24] Gupta, A., Johnson, J., Fei-Fei, L., Savarese, S., and Alahi, A., "Social gan: Socially acceptable trajectories with generative adversarial networks," *Proceedings of the IEEE Conference on Computer Vision and Pattern Recognition*, 2018, pp. 2255–2264.

American Institute of Aeronautics and Astronautics

[25] Sadeghian, A., Kosaraju, V., Sadeghian, A., Hirose, N., Rezatofighi, H., and Savarese, S., "Sophie: An attentive gan for predicting paths compliant to social and physical constraints," *Proceedings of the IEEE/CVF Conference on Computer Vision and Pattern Recognition*, 2019, pp. 1349–1358.

[26] Pang, Y. and Liu, Y., "Conditional generative adversarial networks (CGAN) for aircraft trajectory prediction considering weather effects," *AIAA Scitech 2020 Forum*, 2020, p. 1853.

[27] Wu, J., Zhang, C., Xue, T., Freeman, W. T., and Tenenbaum, J. B., "Learning a probabilistic latent space of object shapes via 3d generative-adversarial modeling," *Proceedings of the 30th International Conference on Neural Information Processing Systems*, 2016, pp. 82–90.

[28] Hochreiter, S. and Schmidhuber, J., "Long short-term memory," *Neural computation*, Vol. 9, No. 8, 1997, pp. 1735–1780.

[29] Goodfellow, I., Pouget-Abadie, J., Mirza, M., Xu, B., Warde-Farley, D., Ozair, S., Courville, A., and Bengio, Y., "Generative adversarial nets," *Advances in neural information processing systems*, Vol. 27, 2014.

[30] Calinon, S., Guenter, F., and Billard, A., "On learning, representing, and generalizing a task in a humanoid robot," *IEEE Transactions on Systems, Man, and Cybernetics, Part B (Cybernetics)*, Vol. 37, No. 2, 2007, pp. 286–298.

[31] Fabisch, A., "gmr: Gaussian Mixture Regression," *Journal of Open Source Software*, Vol. 6, No. 62, 2021, pp. 3054.